Talanta 83 (2010) 139–144

Contents lists available at ScienceDirect

Talanta

journal homepage: www.elsevier.com/locate/talanta

Ultrasensitive mercury(II) ion detection by europium(III)-doped cadmium sulfide composite nanoparticles

Hong-Qi Chen, Jie Fu, Lun Wang*, Bo Ling, Bin-bin Qian, Jing-guo Chen, Cai-ling Zhou

Anhui Key Laboratory of Chemo-Biosensing, College of Chemistry and Materials Science, Anhui Normal University, No. 1 Renmin Road, Wuhu 241000, PR China

ARTICLE INFO

Article history:
Received 4 March 2010
Received in revised form 27 August 2010
Accepted 29 August 2010
Available online 22 September 2010

Keywords:
Fluorescence
Cadmium sulfide nanoparticles
Eu^{3+}
Mercury(II)
Detection

ABSTRACT

With the biomolecule glutathione (GSH) as a capping ligand, Eu^{3+}-doped cadmium sulfide composite nanoparticles were successfully synthesized through a straightforward one-pot process. An efficient fluorescence energy transfer system with CdS nanoparticles as energy donor and Eu^{3+} ions as energy accepter was developed. As a result of specific interaction, the fluorescence intensity of Eu^{3+}-doped CdS nanoparticles is obviously reduced in the presence of Hg^{2+}. Moreover, the long fluorescent lifetime and large Stoke's shift of europium complex permit sensitive fluorescence detection. Under the optimal conditions, the fluorescence intensity of Eu^{3+} at 614 nm decreased linearly with the concentration of Hg^{2+} ranging from 10 nmol L^{-1} to 1500 nmol L^{-1}, the limit of detection for Hg^{2+} was 0.25 nmol L^{-1}. In addition to high stability and reproducibility, the composite nanoparticles show a unique selectivity towards Hg^{2+} ion with respect to common coexisting cations. Moreover, the developed method was applied to the detection of trace Hg^{2+} in aqueous solutions. The probable mechanism of reaction between Eu^{3+}-doped CdS composite nanoparticles and Hg^{2+} was also discussed.

1. Introduction

Mercury is a well-known chemical pollutant derived from both natural and industrial sources. Mercury(II) ion derivative can accumulate in the organs of living things through food chain, doing huge harm to human being and the nature [1,2]. Due to the highly toxic nature of this element in both its inorganic and organic forms, the determination of such low levels of mercury in an aquatic environment is of great importance [3]. A variety of sophisticated analytical techniques have been developed for the detection of Hg^{2+} in real samples. These include X-ray fluorescence spectrometry [4], inductively coupled plasma mass spectrometry [5], electrothermal atomic absorption spectrometry [6], atomic fluorescence spectrometry [7] and cold vapor atomic absorption spectrometry [8]. However, these techniques mostly are time-consuming or require expensive equipment [5,7]. In recent years, the fluorimetric method has been widely used in trace analysis of heavy metal ions due to their high sensitivity, convenient performance and good selectivity [9,10]. Currently, many fluorescent organic probes and sensors such as organic dyes were designed for recognition and detection of Hg^{2+} [11–14]. However, most of these conventional organic fluorescent dyes usually undergo fluorescence quenching effect upon binding of heavy metal ions due to their heavy atom effect, and most of them tend to have narrow excitation spectra and often exhibit broad emission band with red tailing [15]. So it is still a challenge to develop rapid and inexpensive methods with a novel fluorescence material as fluorescence probe for monitoring this dangerous and widespread global pollutant.

Compared to organic fluorophores, rare earth ions exhibit a very narrow emission line and a large excitation–emission separation. Unfortunately, rare earth ions in aqueous solution are known to be either non-fluorescent or weakly fluorescent due to their low molar absorptivities and poor quantum yields [16], direct or indirect band-gap semiconductors could be good sensitizing centers since their excitation cross-sections are very high due to the efficient band-to-band absorptions. It is well known that simple semiconductor nanoparticles (CdS, CdSe, CdTe, etc.) and core/shell quantum dots (CdSe/CdS, CdSe/ZnS, etc.) [17] with high fluorescence quantum yields, high photobleaching threshold and excellent photostability become a new class of fluorescent probes for many biological applications [18–21]. These nanoparticles have generated great research interest in the past two decades for their novel electronic and optical properties [22–24]. So far some reports of chemical sensing of heavy metal ions with semiconductor nanoparticles via spectra changes in photoluminescence have been reported in the literature. Chen and Rosenzweig [25] first reported demonstrated functionalized CdS QDs capped with different organic ligands as luminescent probs for copper and zinc ions. Currently, L-cysteine-capped CdS quantum dots have been synthesized by Chen et al. [26] for the detection of mercury ions, Jin et

* Corresponding author. Tel.: +86 553 5910008; fax: +86 553 5910008.
E-mail address: wanglun@mail.ahnu.edu.cn (L. Wang).

0039-9140/$ – see front matter © 2010 Elsevier B.V. All rights reserved.
doi:10.1016/j.talanta.2010.08.052

al. [27,28] reported the functionalized CdSe QDs as the lunminescence probe for CN^- and CdS QDs for the detection of Hg^{2+}. All these reports reveal that semiconductor nanoparticles as one luminescence probes and sensor were widely studied. Among these, few workers have reported the measurement of mercury(II) ion using semiconductor QDs [29,30,26,31]. Therefore, using functionalized CdS as probe for the detection of mercury(II) ions is still necessary.

Recently, a number of papers reported on the luminescence of nanocrystalline II–VI semiconductors doped with Tb^{3+} [32,33], Sm^{2+} [34], Eu^{3+} [35–37] or Er^{3+} [38]. The enhanced luminescence of rare earth ions was achieved by efficient energy transfer from semiconductor quantum dots to rare earth ions. In various articles it was concluded that the RE-doped II–VI semiconductors nanocrystals "form a new class of luminescent materials" [35]. In recent years, nanocrystalline samples of CdS/Eu or Zn/S were prepared by using a microemulsion technique [36], common precipitation methods [37] and sol–gel processing [37]. However, these methods mostly are time-consuming. Considering this, the Eu^{3+}-doped cadmium sulfide composite nanoparticles were synthesized through a one-pot process was used as a fluorescence probe for determination of mercury ions.

In our work, the Eu^{3+}-doped cadmium sulfide composite nanoparticles were successfully synthesized through a straightforward one-pot process. Moreover, the CdS nanoparticles were modified with GSH which has an important tripeptide with strong affinity to cadmium and the properties of GSH-capped CdS complexes have been reported before [39]. Based on the fact that Hg^{2+}, for being a "soft" metal cation, prefers to strong affinity to RSH- and RS-compounds, the Eu^{3+}-doped CdS composite nanoparticles capped with GSH exhibits an advantage to interact with Hg^{2+}. With CdS nanoparticles as donor and Eu^{3+} ions as accepter, an efficient fluorescence energy transfer system was built. As the energy transfer system can be destroyed upon combining with Hg^{2+}, the fluorescence intensity of both CdS particles and Eu^{3+} ions are obviously reduced in the presence of Hg^{2+}. Among them, Eu^{3+} ions showed preferable fluorescence response to mercury^{2+}. So we chosen Eu complex which has a very large Stoke's shift and long fluorescence lifetime to detect Hg^{2+} ions. From the careful research, it is concluded that this method will enable us to construct efficient RE-doped CdS nanoparticles for heavy metals detection based on fluorescence quenching effect.

2. Experimental

2.1. Apparatus and reagents

The fluorescence spectra were performed using a Hitachi F-4500 spectrofluorometer (Hitachi, Japan) equipped with a plotter unit and a quartz cell (1 cm × 1 cm). The transmission electron microscopy (TEM) images of a JEM-2100 transmission electron microscope (JEOL, Japan). The UV spectra were acquired on a U-3010 spectrofluorometer (Hitachi). All pH values were measured with a pHS-3C digital pH meter (Analytical Instruments Co., Tianda, Shanghai, China).

All chemicals were of analytical-reagent grade or better. The stock solutions of $CdCl_2{\cdot}2.5H_2O$ (Alfa, USA), CH_3CSNH_2 (Alfa), NaOH (Alfa), $HgCl_2$ (Shanghai Reagent Company, China), $EuCl_3{\cdot}6H_2O$ (Sigma), sodium hexametaphosphate (Alfa) and GSH (Alfa) were prepared by dissolving them in ultra pure water without further purification. The phosphoric buffer solution (PBS) was prepared by adjusting 0.067 mol L^{-1} KH_2PO_4 with 0.067 mol L^{-1} Na_2HPO_4. Ultra pure water was used throughout.

2.2. Synthesis of Eu^{3+}-doped CdS composite nanoparticles

The Eu^{3+}-doped CdS nanoparticles were prepared according to the scheme reported in the literatures [40,41] and our previous work for mercaptoacetic acid capped CdS nanocrystals reported by Liang and co-workers [42] with a little change. Briefly, 30 mL 0.01 mol L^{-1} $CdCl_2{\cdot}2.5H_2O$, 60 mL of 0.1 mol L^{-1} sodium hexametaphosphate, 100 mL 0.01 mol L^{-1} GSH and 150 mL 0.01 mol L^{-1} Eu^{3+} were mixed in a 1000 mL three-necked round bottomed flask and purged with N_2 at room temperature. Under vigorous stirring, 150 mL 0.01 mol L^{-1} CH_3CSNH_2 were added drop-wise and then 100 mL 0.1 mol L^{-1} NaOH solutions were added drop-wise to the flask. After stirring for 2 h, the composite nanoparticles were obtained. The as-prepared solutions were stable for 1 month at room temperature, which have not been investigated any visible coacervation or precipitation.

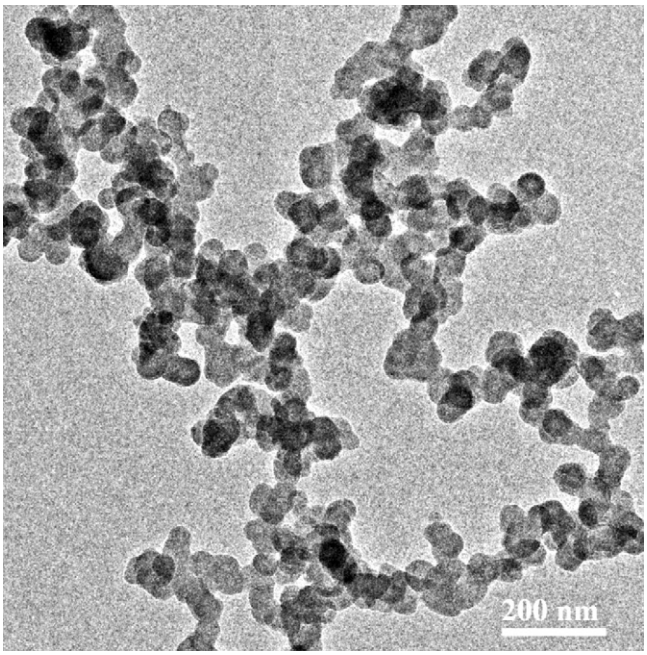

Fig. 1. TEM image of the Eu^{3+}-doped cadmium sulfide composite nanoparticles.

2.3. Procedure of determination of Hg^{2+}

To a 10 mL volumetric flasks, 4 mL of the as-prepared Eu^{3+}-doped CdS solution, 2 mL of PBS (pH 5.3) and various amount of Hg^{2+} were sequentially added. The mixture was then diluted to volume with ultra pure water and mixed thoroughly and incubated for 10 min at room temperature. The fluorescence intensity of the solution was recorded at 614 nm with the excitation wavelength of 395 nm. Both slit widths of excitation and emission were 5 nm.

3. Result and discussion

3.1. TEM image and Spectral characterization of the Eu^{3+}-doped CdS nanoparticles

The morphology of the Eu^{3+}-doped CdS nanoparticles was studied by TEM shown in Fig. 1. The TEM image shows that the observed diameter of the nanoparticles was about 45 nm or so.

Fig. 2 shows the emission spectrum of Eu^{3+} (1), CdS nanoparticles (2) and Eu^{3+}-CdS composite nanoparticles (3). As shown in curve 1 of Fig. 2, the characteristic peaks of Eu^{3+} located at 592, 614 and 698 nm under the excitation wavelength of 395 nm, the three weak peaks are attributed to $^5D_0$-^7F_J. The fluorescence intensity at 614 nm is stronger than that at 592 nm and 698 nm. The fluorescence of CdS nanoparticles without Eu^{3+} (curve 2) was shown in Fig. 2, it can be seen that the strong emission wavelength occurs at

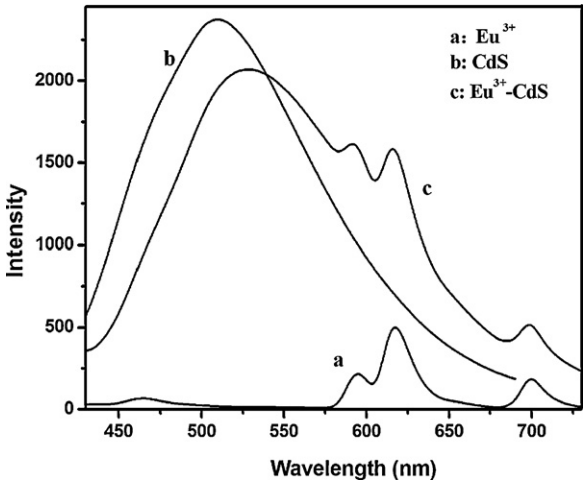

Fig. 2. Emission spectra of (a) Eu^{3+}, 1.0×10^{-3} mol L^{-1}, (b) CdS nanoparticles, 2.0×10^{-4} mol L^{-1}, (c) Eu^{3+}-CdS composite nanoparticles, 2.0×10^{-4} mol L^{-1}, pH 5.3, excitation spectra (λ_{ex} = 395 nm).

510 nm. After doping with Eu^{3+} ions, the fluorescence of Eu^{3+} ion can be enhanced remarkably, which indicates that CdS nanoparticles has the enhancement effect on the luminescence of Eu^{3+}, so the reaction between CdS nanoparticles and Eu^{3+} was studied. We found that the characteristic fluorescence intensity of Eu^{3+} enhanced with the amount of Cd^{2+} increased (Fig. 3). Obviously, there was a fluorescence energy transfer process between CdS nanoparticles and Eu^{3+}. The fluorescence intensity of the Eu^{3+} only changed a little, when the concentration of the Cd^{2+} raised to a certain value. The reason might be that the fluorescence energy transfer efficiency reached to maximum.

As we known that upon excitation of the CdS host, the energy from non-radiative recombination of electron–hole pairs can be transferred to the high-lying energy levels of the Eu^{3+} [43]. When the trace amounts of Hg^{2+} were added to the Eu^{3+}-doped CdS nanoparticles solution, the wavelength of excitation and emission were unchanged, but the intensity of the peak decreased in Fig. 4, the possible mechanism for the fluorescence quenching effect of Eu^{3+} is that the energy transfer system was destroyed upon combining with Hg^{2+}, thus reducing the fluorescence quantum efficiency of the composite nanoparticles. Although the fluorescence intensity of the CdS nanoparticles and Eu^{3+} both decreased in the present

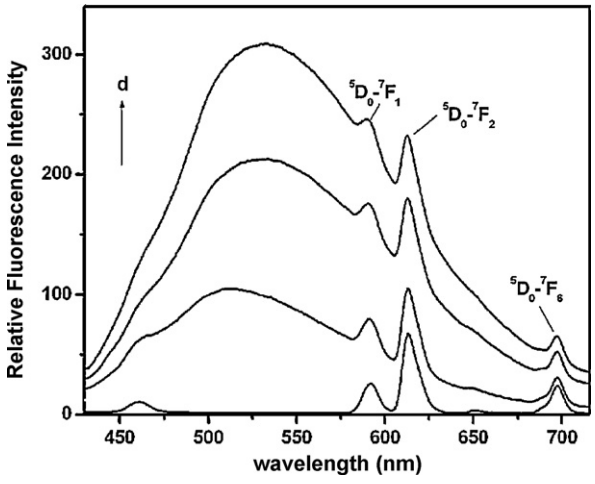

Fig. 3. The fluorescence emission spectra of the Eu^{3+}-doped CdS nanoparticles. Concentration of Cd^{2+} (a) 0.00 mol L^{-1}, (b) 1.0×10^{-4} mol L^{-1}, (c) 2.0×10^{-4} mol L^{-1}, and (d) 3.0×10^{-4} mol L^{-1}, Eu^{3+} (1.0×10^{-3} mol L^{-1}); all in pH 5.3 PBS.

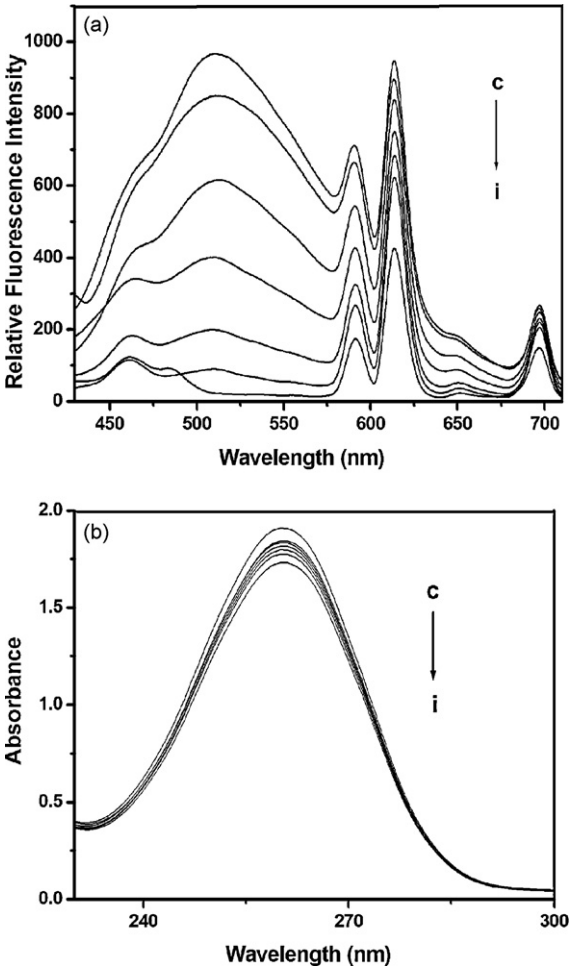

Fig. 4. (a) The fluorescence spectra and (b) absorption spectra of the Eu^{3+}-doped CdS composite nanoparticles (2.0×10^{-4} mol L^{-1}) in the presence of Hg^{2+} at various concentrations (nmol L^{-1}, pH 5.3); (c–i) 0, 60, 300, 500, 700, 900, and 1500, respectively.

of Hg^{2+}, we found that the sensitivity and detection limit of using the characteristic fluorescence of Eu^{3+} for Hg^{2+} detection is better than CdS nanoparticles. Furthermore, the Eu complex has a very large Stoke's shift that permitted more sensitive fluorescence detection, so we chose the characteristic fluorescence of Eu^{3+} ion for the detection of Hg^{2+}.

3.2. Optimum amounts of the Eu^{3+}-doped CdS composite nanoparticles in determination

To investigate the effect of the concentration of the composite nanoparticles solution, a series of calibration functions (the quenched fluorescence intensity against the concentration of Hg^{2+}) were obtained with various concentrations of the Eu^{3+}-doped CdS composite nanoparticles. When Hg^{2+} was added into the lower concentration of composite nanoparticles, the quenching effect of the system was enhanced, with a favorable sensitivity and a narrow linear range, however, with a high concentration of composite nanoparticles there was a low sensitivity and a wide linear range shown in Table 1. The optimal concentration of the Eu^{3+}-doped CdS composite nanoparticles should give attention to both sensitivity and linear range, so 2.0×10^{-4} mol L^{-1} of the aqueous solution was employed for further experiments.

Table 1
Effect of the Eu^{3+}-doped CdS composite nanoparticles in determination of Hg(II).

Concentration of Eu^{3+}-doped CdS with Cd^{2+} as a standard (mol L^{-1})	Linear range (nmol L^{-1})
0.1×10^{-4}	3–250
0.5×10^{-4}	5–650
2.0×10^{-4}	10–1500
3.5×10^{-4}	90–2000
5.0×10^{-4}	500–4500

3.3. Reaction and mixing sequence

The experiments indicated that at room temperature, the reaction between composite nanoparticles and Hg^{2+} reached the equilibrium within 10 min, and the fluorescence intensity remained stable for at least 1 h. In addition, we found that the best order is to mix nanoparticles solution, buffer solution first and then Hg^{2+}, after investigating several adding sequences. Therefore, all the measurements were made after nanoparticles solution, buffer solution and Hg^{2+} were completely mixed for 10 min.

3.4. Effect of pH

The effect of pH value was also investigated from 4.4 to 9.2. As shown in Fig. 5, the pH of the solution has great effect on the fluorescence intensity of the system. It could be seen that $I_{\Delta F}$ ($\Delta F = F_0 - F$) increased with an increase in pH when pH was lower than 5.3, reached maximum when pH was 5.3, and then sharply decreased when pH was above 5.3. To obtain high fluorescence intensity with good precision, a pH of 5.3 was chosen for further research.

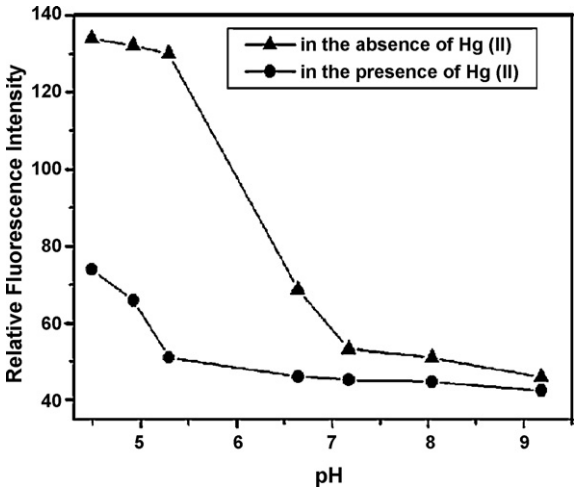

Fig. 5. Effect of pH on the relative fluorescence intensity. Composite nanoparticles: 2.0×10^{-4} mol L^{-1}; Hg^{2+}: 100 nmol L^{-1}.

Table 2
Effect of the interference of coexisting substances.

Coexisting substance[a]	Coexisting concentration (μmol L^{-1})	Relative error (%)
Ca^{2+}	20.0	−0.8
Mg^{2+}	20.0	−1.5
Al^{3+}	10.0	1.9
Fe^{3+}	10.0	−1.3
Mn^{2+}	5.0	−1.7
Ni^{2+}	5.0	−2.6
Zn^{2+}	5.0	−0.7
Cu^{2+}	5.0	−3.0
Ag^{+}	5.0	2.3
Cd^{2+}	5.0	1.8
Pb^{2+}	5.0	−1.4
Ba^{2+}	2.5	2.5
Co^{2+}	2.5	−2.0
Cr^{2+}	2.5	−0.9

[a] Hg^{2+}: 5×10^{-8} mol L^{-1}; composite nanoparticles: 2.0×10^{-4} mol L^{-1}; pH 5.3.

3.5. Interference of coexisting foreign substances

To evaluate the selectivity of this method, the effects of foreign ions on the fluoresence of the Eu^{3+}-doped CdS composite nanoparticles were investigated. At the Hg^{2+} concentration of 50 nmol L^{-1}, the effects of foreign substances causing a relative error in the fluorescence intensity were listed in Table 2. Most of the ions can be allowed at very high concentrations such as Mg^{2+} and Ca^{2+}, while few ions can be allowed at low concentrations, Cu^{2+} shows little quenching of the fluorescence intensity, so a proper amount of acetylacetonate solutions can be used as masking agents to eliminate the interferences from higher concentrations of heavy metal ions [29]. The results indicate that the present method is selective.

3.6. Analytical performance of the Eu^{3+}-doped CdS composite nanoparticles

The fluorescence spectra of the Eu^{3+}-doped CdS composite nanoparticles and its fluorescence titration with Hg^{2+} were recorded. At the optimum experimental conditions, a good linearity between the quenched fluorescence intensity ($\Delta F = F_0 - F$) of the Eu^{3+} and the concentration of Hg^{2+} was observed from 10 nmol L^{-1} to 1500 nmol L^{-1} with a correlation coefficient (γ^2) of 0.9975 and a linear regression equation is $\Delta F = 0.36C$ (nmol L^{-1}) + 12.54. The 3σ limits of detection for Hg^{2+} is 0.25 nmol L^{-1} (here σ represents the standard deviation of eight blank measurements). It is obviously that the sensitivity and detection limit of this method for Hg^{2+} detection using QDs-based sensing systems is better than that of most traditional fluorimetric methods shown in Table 3. It must be noticed that the Eu^{3+}-doped CdS QDs provide better sensitivity towards Hg^{2+} than that of traditional thiol-capped QDs.

To evaluate the potential use of the composite nanoparticles to determine Hg(II) ions in real water samples, an attempt was made to determine Hg(II) ions in tap water, lake water and river water samples, which were filtered three times through qualitative filter paper before use. Each sample was analyzed by standard addition method and also using Cold vapor atomic fluorescence

Table 3
Comparison of the linear range and detection limit of several selected fluorimetric methods for determination of Hg^{2+}.

Reagent	$\lambda_{ex}/\lambda_{em}$ (nm)	Linear range (10^{-7} mol L^{-1})	LOD (10^{-9} mol L^{-1})	Reference
MPA-capped-CdTe	365/535	0–1.28	0.5	[29]
Functionalized CdS QDs	360/495	0.16–1.12	2.4	[30]
dBSA-coated-CdTe	380/541	0.12–15	4.0	[13]
Functionalized CdSe QDs	430/530	0.00–20	6.0	[26]
MAA-capped-CdS	335/460	0.05–4.0	4.2	[31]
Eu^{3+}-doped CdS particles	395/618	0.1–15	0.25	This work

Table 4
Determination of Hg(II) in water samples.

Sample	Certified value (μg/mL)	This method (μg/mL), $n=5$	RSD (%)	Hg(II) added (10^{-9} mol L^{-1})	Hg(II) found (10^{-9} mol L^{-1})[a]		Recovery (%)
					This method	CV-AFS	
GBW(E)080701	0.100	0.103	1.5				
GBW(E)080041	1.00	0.998	2.1				
Tap water				60	64	62	107
				500	516	508	103
River water[b]				60	57	59	95
				500	480	489	96
Lake water[c]				60	63	61	105
				500	520	515	104
Synthetic Hg^{2+}-polluted water[d]				50	47	48	94
				100	96	98	96

[a] The average of five replicate determinations.
[b] River water at Yangtze River, Wuhu.
[c] Lake water at Jinghu, Wuhu.
[d] Synthesized by: 450 nmol L^{-1} of Al(III), 150 nmol L^{-1} of Mn(II), 3000 nmol L^{-1} of Ca(II) and Mg(II), 3.5 nmol L^{-1} of Ag(I) and 5.0 nmol L^{-1} of Pb(II), 3.0 nmol L^{-1} of Cu(II) and Ni(II).

spectrometry (CV-AFS) as a standard method. Two certified reference materials (Mercury in water GBW(E)080701, GBW(E)080041) were selected to analyze by this method. The results are given in Table 4, which shows that the results of recovery for three samples were satisfied and the accuracy also is well, thereby reflecting the utility of the proposed method.

3.7. The probable mechanism of reaction

To understand the interaction between Hg^{2+} and Eu^{3+}-doped CdS nanoparticles, the response characteristics of composite nanoparticles to Hg ions were systematically studied by steady-state fluorescence spectroscopy and UV-vis absorption. As shown in Fig. 5, it can be seen that a significant fluorescence quenching of QDs and the absorption spectra at 260 nm decrease in the presence of mercury ions were observed without any significant shift in the absorption and emission peak. Therefore, we speculated that the experimental phenomenon can be explained in the terms of strong affinity of mercury to nitrogen atom [44] which lead to facilitating non-radiative excited electrons (e^-) in the conduction band and holes (h^+) in the valence band recombination on the surface of QDs through a effective electron transfer process between surface functional amide groups $-NH_2$ and mercury ions [26]. It is known that Isarov and Chysochoos [45] investigated copper ions in quenching the emission of CdS QDs and found that copper ions formed ultra small Cu_xS ($x=1$, 2), the copper ions displaced the Cd^{2+} in the CdS QDs due to its higher binding affinity to S, as indicated by its lower K_{sp} values. It is very interesting to note that the K_{sp} constant of HgS ($K_{sp_{(HgS)}} = 6.4 \times 10^{-53}$) is much lower than that of CuS ($K_{sp_{(CuS)}} = 1.3 \times 10^{-36}$). In the proposed synthesis method, it was formed an amount of sulfide, but there were no obvious precipitation of HgS. The possible reason was HgS precipitate on the surface of the CdS composite nanoparticles. Therefore, it can be speculated that the phenomena of CdS QDs luminescence quenching is because of the fact that electron transfer from surface traps of QDs to Hg^{2+}. Moreover, surface ligands also have profound effects on fluorescence response of QDs to metal ions.

Although the above conclusions provide proof for the proposed quenching mechanisms of the Eu^{3+}, to further verify them, the fluorescence decays were examined. All of the curves can be fitted well with the equation of $I = A + B\exp(-t/\tau)$ as shown in Table 5, these data shows the decreased tendency of τ_1 with an increasing amount of Hg^{2+}, which may result from the ultrafast energy transfer process.

Table 5
The fit results of fluorescence lifetimes before and after quenching of Eu^{3+}-doped CdS QDs.

The sample[a]	$\tau/\mu s$	B	χ^2
1	512.19	133.2	1.241
2	488.54	92.75	1.212
3	437.56	26.37	1.079

[a] Eu^{3+}-doped CdS QDs in the absence and presence of Hg^{2+} ((1) 0.0; (2) 500; (3) 1200 nmol L^{-1}).

4. Conclusions

The water-soluble and biocompatible Eu^{3+}-doped CdS composite nanoparticles capped with GSH were successfully synthesized by using low-cost and green materials. Fluorescence response of Eu^{3+}-doped CdS composite nanoparticles to Hg^{2+} was investigated. The fluorescence quenching phenomenon of Eu^{3+} can be attributed to the fact that local environment for the energy transfer was destroyed upon combining with Hg^{2+}. Based on this, the Eu^{3+}-doped CdS composite nanoparticles can be developed to be a sensitive and identified fluorescence probe for Hg^{2+} detection in aqueous solution. The results suggest that these kinds of rare earth (Eu^{3+}, Te^{3+}, Er^{3+}, Sm^{3+}, etc.) doped semiconductor nanoparticles (CdS, ZnS, etc.), can be used in many fields such as chemical sensors (especially in fiber optic coating platforms [46]), fluorescence probes, and other analytical applications. Further studies with the doped nanoparticles will expand its application in analytical chemistry.

Acknowledgements

This work was supported by Natural Science Foundation of China (20875004, 20905003).

References

[1] A.H. Stern, R.J.M. Hudson, C.W. Shade, S. Ekino, T. Ninomiya, M. Susa, Science 303 (2004) 763–766.
[2] D.W. Boening, Chemosphere 40 (2000) 1335–1351.
[3] M.S. Hoesseini, H.H. Moghaddam, Anal. Sci. 20 (2004) 1449–1452.
[4] L. Bennun, J. Gomez, Spectrochim. Acta B 52 (1997) 1195–1200.
[5] P. Jitaru, F.C. Adams, J. Chromatogr. A 1055 (2004) 197–207.
[6] C. Burrini, A. Cagnini, Talanta 44 (1997) 1219–1223.
[7] S. Diez, J.M. Bayona, J. Chromatogr. A 963 (2002) 345–351.
[8] Y. Yamini, N. Alizadeh, M. Shamsipur, Anal. Chim. Acta 355 (1997) 69–74.
[9] R.H. Yang, Y. Zhang, K.A. Li, F. Liu, W.H. Chan, Anal. Chim. Acta 525 (2004) 97–103.
[10] M.T. Fernández-Argüelles, W.J. Jin, J.M. Costa-Fernández, R. Pereiro, A. Sanz-Medel, Anal. Chim. Acta 549 (2005) 20–25.

[11] E.M. Nolan, S.J. Lippard, J. Am. Chem. Soc. 125 (2003) 14270–14271.
[12] Y.K. Yang, K.Y. Yook, J.S. Tae, J. Am. Chem. Soc. 127 (2005) 16760–16761.
[13] Y.S. Xia, C.Q. Zhu, Talanta 75 (2008) 215–221.
[14] H. Zheng, Z.H. Qian, L. Xu, F.F. Yuan, L.D. Lan, J.G. Xu, Org. Lett. 8 (2006) 859–861.
[15] H. Mattoussi, J.M. Manro, E.R. Goldman, G.P. Anderson, V.C. Sunder, F.V. Mikula, M.G. Bawendi, J. Am. Chem. Soc. 122 (2000) 12142–12150.
[16] Y.X. Zheng, J. Lin, Y.J. Liang, H.J. Zhang, Mater. Lett. 54 (2002) 424–429.
[17] L.C. Charina, J.K. Kristie, S. Sanjeevi, A.P. Alivisatos, Nano Lett. 9 (2009) 3544–3549.
[18] M.B.M. Moronne Jr., P. Gin, S. Weiss, A.P. Alivisatos, Science 281 (1998) 2013–2016.
[19] W.C.W. Chan, D.J. Maxwell, X.H. Gao, R.E. Bailey, M.Y. Han, S.M. Nie, Curr. Opin. Biotechnol. 13 (2002) 40–46.
[20] S. Kim, B. Fisher, H.J. Eisler, M. Bawendi, J. Am. Chem. Soc. 125 (2003) 11466–11467.
[21] S.W. Kim, J.P. Zimmer, S. Ohnishi, J.B. Tracy, J.V. Rangioni, M.G. Bawendi, J. Am. Chem. Soc. 127 (2005) 10526–10532.
[22] H. Qian, C. Dong, J. Weng, J. Ren, Small 2 (2006) 747–751.
[23] R. Yang, Y. Yan, Y. Mu, W. Ji, X. Li, M. Zhou, Q. Fei, Q. Jin, J. Nanosci. Nanotechnol. 6 (2006) 215–220.
[24] Y. Zheng, S. Gao, J.Y. Ying, Adv. Mater. 19 (2007) 376–380.
[25] Y.F. Chen, Z. Rosenzweig, Anal. Chem. 74 (2002) 5132–5138.
[26] J.L. Chen, Y.C. Gao, Z.B. Xu, G.H. Wu, Y.C. Chen, C.Q. Zhu, Anal. Chim. Acta 577 (2006) 77–84.
[27] W.J. Jin, J.M. Costa-Fernandez, R. Pereiro, A. Sanz-Medel, Anal. Chim. Acta 522 (2004) 1–8.
[28] Z.X. Cai, H. Yang, Y. Zhang, X.P. Yan, Anal. Chim. Acta 559 (2006) 234–239.
[29] B. Chen, Y. Yu, Z. Zhou, P. Zhong, Chem. Lett. 33 (2004) 1608–1609.
[30] X.P. Yan, Z.X. Cai, H. Yang, Y. Zhang, Anal. Chim. Acta 559 (2006) 234–239.
[31] K. Masilamany, N. Ramaier, Sens. Actuator B: Chem. 139 (2009) 91–96.
[32] C. Tiseanu, R.K. Mehra, R. Kho, J. Photochem. Photobiol. A: Chem. 173 (2005) 169–173.
[33] C. Tiseanu, R.K. Mehra, R. Kho, M. Kumke, J. Phys. Chem. B 107 (2003) 12153–12160.
[34] T. Kushida, A. Kurita, M. Watanabe, Y. Kanematsu, J. Lumin. 87–89 (2000) 466–468.
[35] S.J. Xu, S.J. Chua, B. Liu, L.M. Gan, C.H. Chew, G.Q. Xu, Appl. Phys. Lett. 73 (1998) 478–480.
[36] W. Chen, J.O. Malm, V. Zwiller, Y. Huang, S. Liu, R. Wallenberg, J.O. Bovin, L. Samuelson, Phys. Rev. B 61 (2000) 11021–11024.
[37] M. Morita, D. Rau, H. Fujii, Y. Minami, S. Murakami, M. Baba, M. Yoshita, H. Akiyama, J. Lumin. 87–89 (2000) 478–481.
[38] D.Q. Chen, Y.S. Wang, E. Ma, F. Bao, Y.L. Yu, Scr. Mater. 55 (2006) 891–894.
[39] W. Bae, R.K. Mehra, J. Inorg. Biochem. 69 (1998) 33–43.
[40] H. Liu, W.Y. Li, H.Z. Yin, X.W. He, L.X. Chen, Acta Chim. Sin. 63 (2005) 301–306.
[41] L. Wang, Y. Liu, H.Q. Chen, A.N. Liang, F.G. Xu, Chin. Chem. Lett. 18 (2007) 369–372.
[42] L. Wang, A.N. Liang, H.Q. Chen, Y. Liu, B.B. Qian, J. Fu, Anal. Chim. Acta 616 (2008) 170–176.
[43] P.S. Chowdhury, A. Patra, Phys. Chem. Chem. Phys. 8 (2006) 1329–1334.
[44] M.Y. Chae, A.W. Czarmik, J. Am. Chem. Soc. 114 (1992) 9704–9705.
[45] A.V. Isarov, J. Chrysochoos, Langmuir 13 (1997) 3142–3149.
[46] F.J. Steemers, D.R. Walt, Mikrochim. Acta 131 (1999) 99–105.